symmetry

MDPI

Article

Toward Enhanced Geological Analysis: A Novel Approach Based on Transmuted Semicircular Distribution

Phani Yedlapalli [1], Gajula Naveen Venkata Kishore [2], Wadii Boulila [3,*], Anis Koubaa [3] and Nabil Mlaiki [4]

[1] Department of Mathematics, Shri Vishnu Engineering College for Women(A), Bhimavaram 534202, India; phani.maths@svecw.edu.in or phaniyedlapalli23@gmail.com
[2] Department of Engineering Mathematics and Humanities, SRKR Engineering College, Bhimavaram 534204, India; gnvkishore@srkrec.ac.in or kishore.apr2@gmail.com
[3] Robotics and Internet-of-Things Laboratory, Prince Sultan University, Riyadh 11586, Saudi Arabia; akoubaa@psu.edu.sa
[4] Department of Mathematics and Sciences, Prince Sultan University, Riyadh 11586, Saudi Arabia; nmlaiki@psu.edu.sa or nmlaiki2012@gmail.com
* Correspondence: wboulila@psu.edu.sa

Abstract: This paper introduces a novel semicircular distribution obtained by applying the quadratic rank transmutation map to the stereographic semicircular exponential distribution, referred to as the transmuted stereographic semicircular exponential distribution (*TSSCED*). This newly proposed distribution exhibits enhanced flexibility compared to the baseline stereographic semicircular exponential distribution (*SSCEXP*). We conduct a comprehensive analysis of the model's properties and demonstrate its efficacy in data modeling through the application to a real dataset.

Keywords: axial data; characteristics; stereographic projection; semicircular model; transmutation; quadratic rank transmutation map

MSC: 60E05; 62H11

Citation: Yedlapalli, P.; Kishore, G.N.V.; Boulila, W.; Koubaa, A.; Mlaiki, N. Toward Enhanced Geological Analysis: A Novel Approach Based on Transmuted Semicircular Distribution. *Symmetry* **2023**, *15*, 2030. https://doi.org/10.3390/sym15112030

Academic Editors: Calogero Vetro, Siliang Tang and Sunil Kumar

Received: 3 September 2023
Revised: 21 October 2023
Accepted: 29 October 2023
Published: 8 November 2023

1. Introduction

Several innovative distributions have emerged by leveraging fundamental probabilistic concepts, such as cumulative distribution functions (CDFs) [1–3], probability density functions (PDFs), and survival functions. The intention is to introduce enhanced flexibility and encompass a wider spectrum of behaviors compared to the original distributions. Marshall and Olkin in [4] introduced an intriguing method to enhance existing distributions with an extra parameter, resulting in what is known as the Marshall–Olkin extended distributions (MO-distributions). These extended distributions include the original distributions as special cases. This concept of extending distributions, often referred to as "transmutation", was formulated through the utilization of the Quadratic Rank Transmutation Map (QRTM) introduced by Shaw and Buckley in [5]. Consequently, this led to the exploration of transmuted distributions by various researchers.

For instance, Merovci in [6] introduced a transmuted Lindley distribution and applied it to a dataset related to bladder cancer. Merovci et al. in [7] then extended their research by proposing and analyzing properties of the transmuted Lindley-geometric distribution. Another contribution by Sibel Acik Kemaloglu et al. in [8] involved the introduction and examination of diverse properties of the transmuted two-parameter Lindley distribution.

In the realm of circular distributions, researchers have successfully adapted existing probabilistic models from the real line or plane to create a variety of valuable and captivating circular models. Techniques involve wrapping linear models around a circle and focusing on properties such as maximum entropy or applying inverse stereographic projection (S Rao Jammalamadaka et al. in [9–11]). Abe et al. [12] discussed a four-parameter

family of symmetric unimodal distributions that extended both the Minh–Farnum in [13] and Jones–Pewsey in [14] families. Phani et al. in [15] introduced and examined properties of stereographic semicircular exponential and Weibull distributions through inverse stereographic projection on linear exponential and Weibull variables. Rao et al. in [16] developed circular distributions using wrapping techniques and inverse stereographic projection on linear distributions. Arnold et al. in [17] focused on the construction and inference of axial distributions, with a particular emphasis on the axial normal distribution. Rambli et al. in [18] introduced a novel semicircular distribution through inverse stereographic projection applied to a gamma distribution. Building upon this, Ali H. Abuzaid in [19] created a semicircular distribution based on inverse stereographic projection applied to the Burr XII distribution variable.

More recently, Rambli et al. in [20] demonstrated the utility of the half-circular gamma distribution in modeling eye data from a glaucoma clinic. Abdullah Yilmaz et al. in [21] introduced a wrapped exponential distribution using the transmuted rank quadratic map method. Additionally, P. Yedlapalli et al. in [22,23] developed several semicircular models by modifying inverse stereographic projection on linear models. In a recent contribution, Phani et al. in [24] proposed a new family of semicircular and circular arc tan-exponential type distributions, investigating various population characteristics. Furthermore, Ayesha Iftikhar et al. in [25] introduced a modified half-circular Burr-III distribution and explored different estimation methods.

In this study, we aim to formulate a novel distribution by employing the quadratic rank transmutation map on the stereographic semicircular exponential distribution introduced by Phani et al. in [15]. We refer to this distribution as the "transmuted stereographic semicircular exponential distribution" (TSSCED). The novelty of this study is that no researcher so far has studied this technique for semicircular distributions. This newly developed distribution offers greater flexibility compared to the baseline stereographic semicircular exponential distribution (SSCEXP) and other established models in the literature. Our subsequent focus involves an analysis of the properties of the proposed model. While some existing models relate to axial distribution, assuming equivalence between angles (Alldredge et al. [26] and Mardia et al. in [27]), our interest lies in deriving a distribution for observations confined to a semicircle, within the range of $(0, \pi)$ radians. It is important to note that the periodicity property applicable to circular data does not hold for semicircular data, as it is distinctly different.

The rest of this article is structured as follows: Section 2 outlines the transmuted stereographic semicircular exponential distribution. Section 3 derives the trigonometric moments of the proposed model, followed by parameter estimation through the maximum likelihood method in Section 4. Section 5 presents the results of a simulation study. This article also features a practical example involving the orientation of pebbles dataset (Fisher B-8), specifically the horizontal axes of 100 outwash pebbles from a late Wisconsin outwash terrace near Cary, Illinois, in Section 6. Finally, Section 7 offers concluding remarks.

2. Definition and Derivation of the Proposed Model

Let F_1 and F_2 be two distribution functions with a common sample space. The general rank transmutation is defined by Shaw and Buckley [5] as $G_{R12} = F_2(F_1^{-1}(u))$, $u \in [0,1]$, $G_{R21} = F_1(F_2^{-1}(u))$, where $F^{-1}(\tau) = inf_{x \in R}\{F(x) \geq \tau\}$, $\tau \in [0,1]$.

Hence, a quadratic rank transmutation map has the following form: $G_{Rij}(u) = u + \alpha(1-u)$, $-1 \leq \alpha \leq 1$, $u \in [0,1]$. From this transmutation, it follows that F_1 and F_2 satisfy the relationship

$$G_{Rij}(F_i(x)) = F_{(i}(x) + \alpha F_i(x)(1 - F_i(x)) \text{ or } F_j(x) = (1+\alpha)F_i(x) - \alpha F_i^2. \quad (1)$$

The aforementioned equation produces a transformed distribution (F_j) for F_i. When F_1 and F_2 are both continuous distributions, applying the derivative operation to Equation (1) yields the resulting transmuted probability density function.

$$f_j(x) = (1+\alpha)f_i(x) - 2\alpha f_i(x)F_i(x), j = 1 \text{ or } 2, i = 1 \text{ or } 2, i \neq j). \tag{2}$$

If the cumulative distribution function $F(x)$ of the random variable X adheres to the subsequent relation, then X is characterized as having a transmuted distribution:

$$F(x) = (1+\alpha)G(x) - \alpha[G(x)]^2, -1 \leq \alpha \leq 1, \tag{3}$$

where G(x) is cdf of base line distribution.

The parameter α is called a transmutation parameter. By adopting the above methodology to circular distributions, we construct a new distribution called transmuted stereographic semicircular exponential distribution.

A circular random variable θ is said to have the transmuted distribution if its cdf $G(\theta)$ and pdf $g(\theta)$, where $\theta \in (0, 2\pi]$, given by

$$G(\theta) = (1+\alpha)F(\theta) - \alpha[F(\theta)]^2 \tag{4}$$

$$g(\theta) = f(\theta)[(1+\alpha) - 2\alpha F(\theta)], \tag{5}$$

where $-1 \leq \alpha \leq 1$, $F(\theta)$ and $f(\theta)$ are cdf and pdf to the base distribution, respectively. Observe that when $\alpha = 0$, we obtain the base distribution of the random variable θ.

Lemma 1. *$g(\theta)$, given in Equation (5), is a well-defined circular probability density function.*

Proof. A function $g(\theta)$ is said to be a circular probability density function if and only if
(i) $g(\theta) \geq 0, \theta \in (0, 2\pi]$,
(ii) $g(\theta + 2\pi) = g(\theta)$,
(iii) $\int_0^{2\pi} g(\theta)d\theta = 1$.

By rewriting $g(\theta)$ as $g(\theta) = f(\theta)[1 - \alpha(2F(\theta) - 1)]$, we noticed that $g(\theta)$ is non-negative and

$$\begin{aligned} g(\theta + 2\pi) &= f(\theta + 2\pi)\,[(1+\alpha) - 2\alpha F(\theta + 2\pi)] \\ &= f(\theta)\,[(1+\alpha) - 2\alpha F(\theta)] = g(\theta) \text{ (since f}(\theta) \text{ is periodic with period } 2\,\pi\,). \end{aligned}$$

We need to show that the integration over the support of the random variable θ is 1. We have

$$\begin{aligned} \int_0^{2\pi} g(\theta)d\theta &= \int_0^{2\pi} f(\theta)[(1+\alpha) - 2\alpha G(\theta)]d\theta \\ &= (1+\alpha)\int_0^{2\pi} f(\theta)d\theta - \alpha\int_0^{2\pi} 2f(\theta)G(\theta)d\theta \\ &= (1+\alpha)(1) - \alpha(1)(\text{since}\int_0^{2\pi} f(\theta)d\theta = 1\ \&\ \int_0^{2\pi} 2f(\theta)G(\theta)d\theta = 1) \\ &= (1+\alpha) - \alpha = 1. \end{aligned}$$

Similarly, in the case of a semicircle, the support of the random variable is a half part of the circle, i.e., $\theta \in (0, \pi)$ follows, except the periodicity condition.

Using the above methodology, we can develop new circular and semicircular distributions, which are more flexible than the base distributions. □

Transmuted stereographic semicircular exponential distribution (TSSCED)

The cumulative distribution function (cdf) of the stereographic semicircular exponential distribution (Phani et al. [15]) is given by

$$F(\theta) = 1 - \exp\left(-\lambda \tan\left(\frac{\theta}{2}\right)\right), 0 < \theta < \pi, \lambda > 0, \tag{6}$$

and the probability density function (pdf) is given by

$$f(\theta) = \frac{\lambda}{(1+\cos\theta)} \exp\left(-\lambda \tan\left(\frac{\theta}{2}\right)\right), 0 < \theta < \pi, \lambda > 0. \tag{7}$$

From (6) in Equation (4), we obtain the cdf of the transmuted stereographic semicircular exponential distribution (TSSCED).

The the cdf of the TSSCED is given by

$$G(\theta) = (1+\alpha)\left[1 - \exp\left(-\lambda \tan\left(\frac{\theta}{2}\right)\right)\right] - \alpha\left[1 - \exp\left(-\lambda \tan\left(\frac{\theta}{2}\right)\right)\right]^2, \tag{8}$$

where $0 < \theta < \pi$, $\lambda > 0$ and $|\alpha| \leq 1$.

Hence, the pdf of TSSED with parameters α and λ is given as

$$g(\theta; \alpha, \lambda) = \frac{\lambda(1-\alpha)}{(1+\cos\theta)} \exp\left(-\lambda \tan\left(\frac{\theta}{2}\right)\right) + \alpha\lambda \sec^2\left(\frac{\theta}{2}\right) \exp\left(-2\lambda \tan\left(\frac{\theta}{2}\right)\right), \tag{9}$$

where $0 < \theta < \pi$, $\lambda > 0$ and $|\alpha| \leq 1$.

It extends the concept of the stereographic semicircular exponential distribution proposed by Phani et al. [15]. Figures 1–3 illustrate the variation in the probability density function (pdf) and cumulative distribution function (cdf) of the newly introduced model for distinct parameter values. Conversely, Figure 4 provides a circular representation of the proposed model. In Figure 5 we present the survival function of TSSCED for various values of λ. In Figure 6 we provide the plots of hazard rate function of TSSCED for various values of λ.

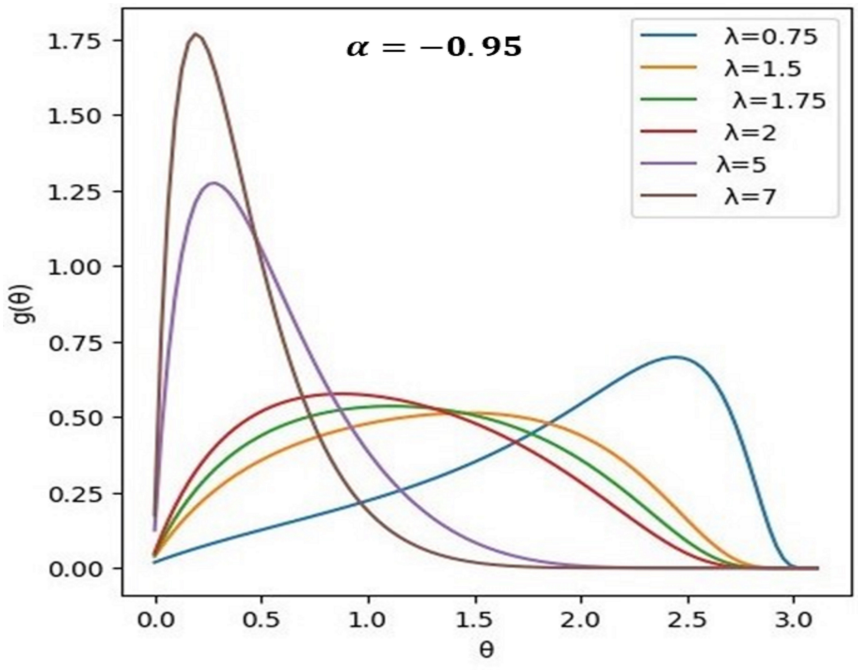

Figure 1. The probability density functions of TSSCED for various values of λ. From these plots it is evident that TSSCD is applicable for both positively and negatively skewed data.

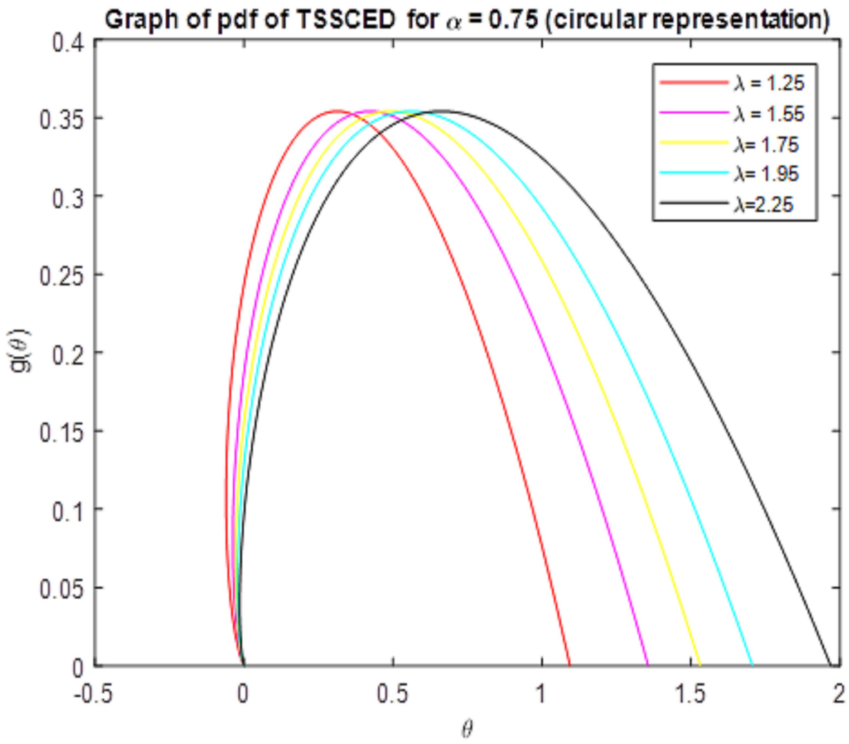

Figure 2. Density plot of TSSCED for various values of λ (circular plot).

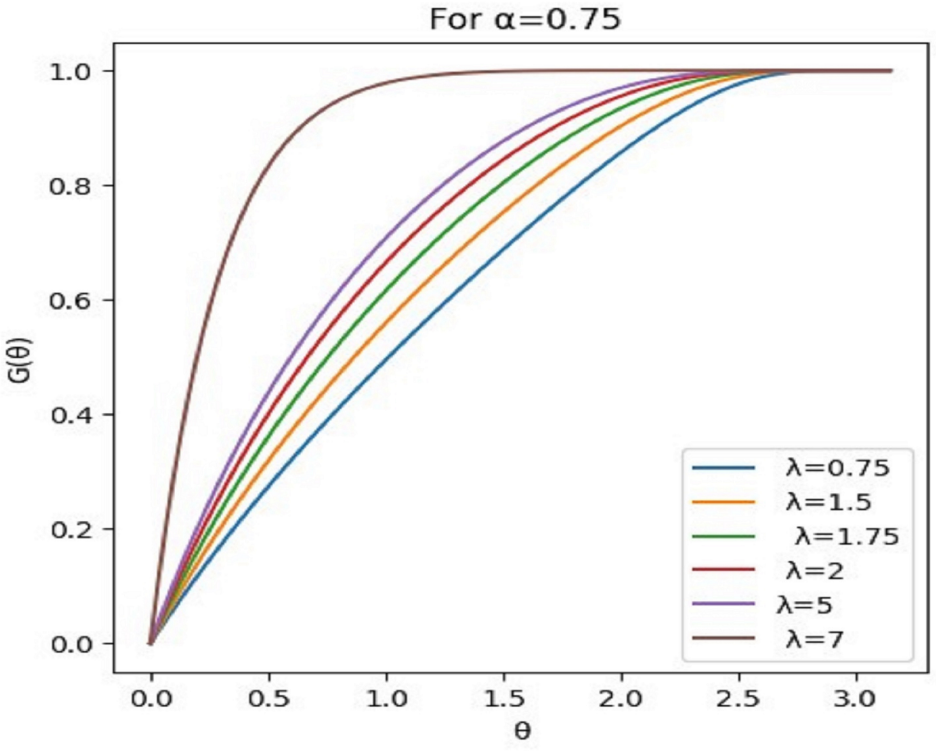

Figure 3. Distribution function plot of TSSCED for various values of λ.

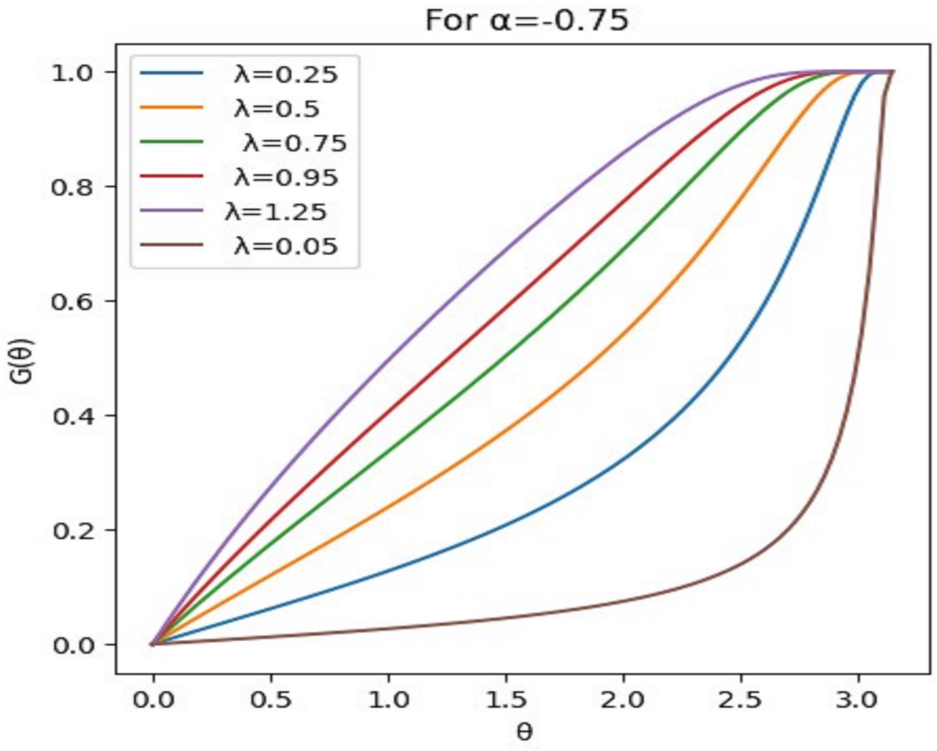

Figure 4. Distribution function plots of TSSCED for various values of λ.

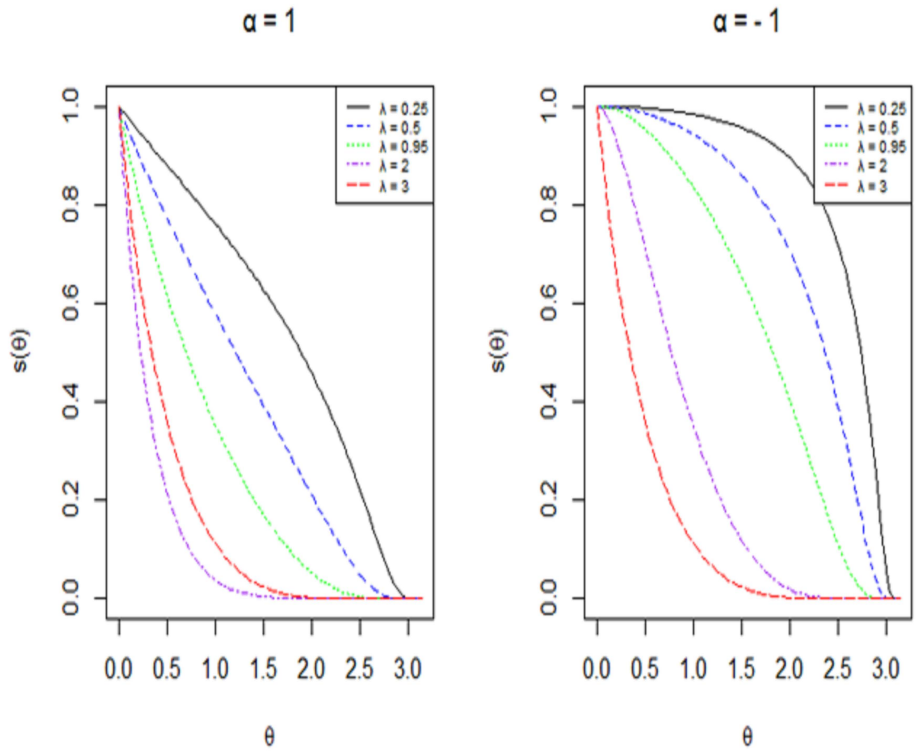

Figure 5. Plots of survival function of TSSCED for various values of λ.

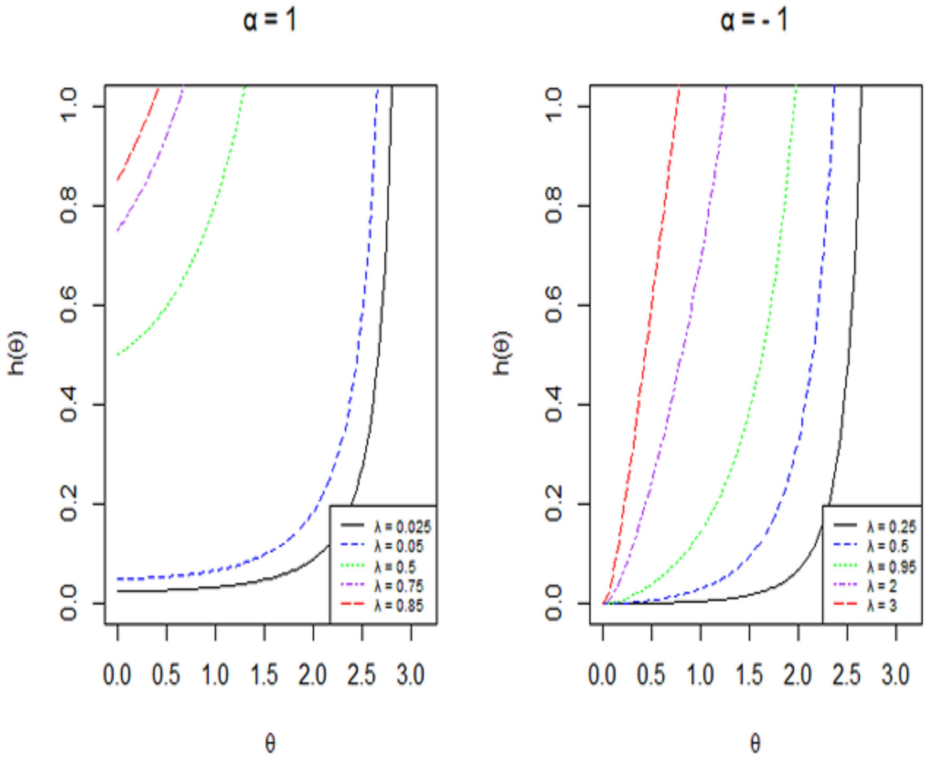

Figure 6. Plots of hazard rate function of TSSCED for various values of λ.

Quantile Function

The quantile function of TSSCED (λ, α) can be obtained from the solution of equation $G(\theta) - u = 0$ with respect to θ as

$$Q(u) = 2\tan^{-1}\left(\frac{1}{\lambda}\log\left(\frac{2\alpha}{\left((\alpha+1) - \sqrt{(\alpha+1)^2 - 4\alpha u}\right)}\right)\right), where \ \ u \in (0,1). \tag{10}$$

The median direction of a semicircular distribution is a value M such that

$$\int_0^M g(\theta)d\theta = \int_M^\pi g(\theta)d\theta = 0.5.$$

The median of the TSSCED (λ, α) distribution is obtained from equation

$$M = Q(0.5) = 2\tan^{-1}\left(\frac{1}{\lambda}\log\left(\frac{2\alpha}{\left((\alpha+1) - \sqrt{(\alpha+1)^2 - 2\alpha}\right)}\right)\right). \tag{11}$$

3. Characteristic Function

The characteristic function of a random angle θ can be represented as the sequence of complex numbers $\{\varphi_p : \ p = \pm 1, \pm 2, \pm 3, \cdots\}$ arranged in a doubly-infinite manner. This sequence is defined by:

$$\begin{aligned}\varphi_p &= E\left(e^{ip\theta}\right) = \int_0^{\pi} e^{ip\theta} d(G(\theta)) \\ &= \frac{\lambda}{2}\int_0^{\pi} e^{ip\theta}\sec^2\left(\frac{\theta}{2}\right)e^{-\lambda\tan\left(\frac{\theta}{2}\right)}\left[(1+\alpha)-2\alpha\left(1-e^{-\lambda\tan\left(\frac{\theta}{2}\right)}\right)\right]d\theta.\end{aligned}$$

As this integral cannot admit an explicit form, we derive the first two trigonometric moments, which are enough for studying population characteristics.

The Trigonometric Moments

We compute the initial two trigonometric moments of the transmuted stereographic semicircular exponential distribution, which are crucial for calculating population characteristics. These moments are represented by the sequence of complex numbers $\{\varphi_p : p = \pm1, \pm2, \pm3, \cdots\}$, where $\varphi_p = \alpha_p + i\beta_p$ and $\alpha_p = E(\cos p\Theta)$ and $\beta_p = E(\sin p\Theta)$ denote the pth order cosine and sine moments, respectively, of the random variable Θ. These moments are essential for subsequent population characteristics calculations.

Theorem 1. *Under the pdf of the transmuted stereographic semicircular exponential distribution, the first two trigonometric moments $\alpha_p = E(\cos p\Theta)$ and $\beta_p = E(\sin p\Theta)$, $p = 1, 2$ are given as follows:*

$$\alpha_1 = 1 - \frac{\lambda}{\sqrt{\pi}}\left[(1-\alpha)\,G_{13}^{31}\left(\frac{\lambda^2}{4}\,\middle|\,\begin{matrix}-\frac{1}{2}\\0,\,0,\,\frac{1}{2}\end{matrix}\right) + 2\alpha G_{13}^{31}\left(\lambda^2\,\middle|\,\begin{matrix}-\frac{1}{2}\\0,\,0,\,\frac{1}{2}\end{matrix}\right)\right]$$

$$\beta_1 = \frac{\lambda}{\sqrt{\pi}}\left[(1-\alpha)\,G_{13}^{31}\left(\frac{\lambda^2}{4}\,\middle|\,\begin{matrix}0\\0,\,0,\,\frac{1}{2}\end{matrix}\right) + 2\alpha G_{13}^{31}\left(\lambda^2\,\middle|\,\begin{matrix}0\\0,\,0,\,\frac{1}{2}\end{matrix}\right)\right]$$

$$\begin{aligned}\alpha_2 &= 1 + \frac{4\lambda(1-\alpha)}{\sqrt{\pi}}\left[G_{13}^{31}\left(\frac{\lambda^2}{4}\,\middle|\,\begin{matrix}-\frac{3}{2}\\-\frac{1}{2},\,0,\,\frac{1}{2}\end{matrix}\right) - G_{13}^{31}\left(\frac{\lambda^2}{4}\,\middle|\,\begin{matrix}-\frac{1}{2}\\-\frac{1}{2},\,0,\,\frac{1}{2}\end{matrix}\right)\right] \\ &\quad + \frac{8\alpha\lambda}{\sqrt{\pi}}\left[G_{13}^{31}\left(\lambda^2\,\middle|\,\begin{matrix}-\frac{3}{2}\\-\frac{1}{2},\,0,\,\frac{1}{2}\end{matrix}\right) - G_{13}^{31}\left(\lambda^2\,\middle|\,\begin{matrix}-\frac{1}{2}\\-\frac{1}{2},\,0,\,\frac{1}{2}\end{matrix}\right)\right],\end{aligned}$$

$$\begin{aligned}\beta_2 &= \frac{2(1-\alpha)\lambda}{\sqrt{\pi}}\left[G_{13}^{31}\left(\frac{\lambda^2}{4}\,\middle|\,\begin{matrix}0\\0,\,0,\,\frac{1}{2}\end{matrix}\right) - 2G_{13}^{31}\left(\frac{\lambda^2}{4}\,\middle|\,\begin{matrix}-1\\0,\,0,\,\frac{1}{2}\end{matrix}\right)\right] \\ &\quad + \frac{4\alpha\lambda}{\sqrt{\pi}}\left[G_{13}^{31}\left(\lambda^2\,\middle|\,\begin{matrix}0\\0,\,0,\,\frac{1}{2}\end{matrix}\right) - 2G_{13}^{31}\left(\lambda^2\,\middle|\,\begin{matrix}-1\\0,\,0,\,\frac{1}{2}\end{matrix}\right)\right].\end{aligned}$$

Proof. The verification involves employing certain transformations. To begin with, for the initial cosine and sine moments, use the transformation $x = \tan\left(\frac{\theta}{2}\right)$, $\cos\theta = 1 - \frac{2x^2}{1+x^2}$ and $\sin\theta = \frac{2x}{1+x^2}$; the results α_1 and β_1 follow by the integral formula 3.389.2 Gradshteyn and Ryzhik in [28].

$$\begin{aligned}
\alpha_1 &= \int_0^{\pi} \cos(\theta) g(\theta) d\theta \\
&= \int_0^{\pi} cos(\theta) \sec^2\left(\frac{\theta}{2}\right) e^{-\lambda \tan\left(\frac{\theta}{2}\right)} \left[\frac{\lambda(1-\alpha)}{2} + 2\lambda e^{-\lambda \tan\left(\frac{\theta}{2}\right)}\right] d\theta \\
&= \int_0^{\infty} \left(1 - \frac{2x^2}{1+x^2}\right) \left[(1-\alpha)\lambda e^{-\lambda x} + 2\alpha\lambda e^{-2\lambda x}\right] dx \\
&= 1 - \left[2(1-\alpha)\lambda \int_0^{\infty} x^{2\left(\frac{3}{2}\right)-1} \left(1+x^2\right)^{0-1} e^{-\lambda x} dx + 4\alpha\lambda \int_0^{\infty} x^{2\left(\frac{3}{2}\right)-1} \left(1+x^2\right)^{0-1} e^{-2\lambda x} dx\right].
\end{aligned}$$

Therefore,

$$\alpha_1 = 1 - \frac{\lambda}{\sqrt{\pi}} \left[(1-\alpha)\, G_{13}^{31}\left(\frac{\lambda^2}{4} \,\middle|\, \begin{matrix} -\frac{1}{2} \\ 0,\, 0,\, \frac{1}{2} \end{matrix}\right) + 2\alpha G_{13}^{31}\left(\lambda^2 \,\middle|\, \begin{matrix} -\frac{1}{2} \\ 0,\, 0,\, \frac{1}{2} \end{matrix}\right)\right]$$

$$\begin{aligned}
\beta_1 &= \int_0^{\pi} sin(\theta) g(\theta) d\theta \\
&= \int_0^{\pi} sin(\theta) \sec^2\left(\frac{\theta}{2}\right) e^{-\lambda \tan\left(\frac{\theta}{2}\right)} \left[\frac{\lambda(1-\alpha)}{2} + 2\lambda e^{-\lambda \tan\left(\frac{\theta}{2}\right)}\right] d\theta \\
&= \int_0^{\infty} \left(\frac{2x}{1+x^2}\right) \left[(1-\alpha)\lambda e^{-\lambda x} + 2\alpha\lambda e^{-2\lambda x}\right] dx \\
&= 2(1-\alpha)\lambda \int_0^{\infty} x^{2(1)-1} \left(1+x^2\right)^{0-1} e^{-\lambda x} dx + 4\alpha\lambda \int_0^{\infty} x^{2(1)-1} \left(1+x^2\right)^{0-1} e^{-2\lambda x} dx.
\end{aligned}$$

Therefore,

$$\beta_1 = \frac{\lambda}{\sqrt{\pi}} \left[(1-\alpha)\, G_{13}^{31}\left(\frac{\lambda^2}{4} \,\middle|\, \begin{matrix} 0 \\ 0,\, 0,\, \frac{1}{2} \end{matrix}\right) + 2\alpha G_{13}^{31}\left(\lambda^2 \,\middle|\, \begin{matrix} 0 \\ 0,\, 0,\, \frac{1}{2} \end{matrix}\right)\right].$$

To obtain the second cosine and sine moments, α_2 and β_2, we use the transformations $x = \tan\left(\frac{\theta}{2}\right)$, $\cos 2\theta = 1 - \frac{8x^4}{(1+x^2)^2} - \frac{8x^2}{(1+x^2)}$, and $\sin 2\theta = \frac{4x}{1+x^2} - \frac{8x^3}{(1+x^2)^2}$; the results of α_2 and β_2 follow from the same integral formula of α_1.

$$\begin{aligned}
\alpha_2 &= \int_0^{\pi} \cos(2\theta) g(\theta) d\theta \\
&= \int_0^{\pi} cos(2\theta) \sec^2\left(\frac{\theta}{2}\right) e^{-\lambda \tan\left(\frac{\theta}{2}\right)} \left[\frac{\lambda(1-\alpha)}{2} + 2\lambda e^{-\lambda \tan\left(\frac{\theta}{2}\right)}\right] d\theta \\
&= \int_0^{\infty} \left(1 + \frac{8x^4}{(1+x^2)^2} - \frac{4x^3}{(1+x^2)}\right) \left[(1-\alpha)\lambda e^{-\lambda x} + 2\alpha\lambda e^{-2\lambda x}\right] dx \\
&= 1 + 8(1-\alpha)\lambda \left[\int_0^{\infty} x^{2\left(\frac{5}{2}\right)-1} \left(1+x^2\right)^{-1-1} e^{-\lambda x} dx - \int_0^{\infty} x^{2\left(\frac{3}{2}\right)-1} \left(1+x^2\right)^{0-1} e^{-\lambda x} dx\right] \\
&\quad + 16\alpha\lambda \left[\int_0^{\infty} x^{2\left(\frac{5}{2}\right)-1} \left(1+x^2\right)^{-1-1} e^{-2\lambda x} dx - \int_0^{\infty} x^{2\left(\frac{3}{2}\right)-1} \left(1+x^2\right)^{0-1} e^{-2\lambda x} dx\right]
\end{aligned}$$

$$\begin{aligned}
\alpha_2 &= 1 + \frac{4\lambda(1-\alpha)}{\sqrt{\pi}} \left[G_{13}^{31}\left(\frac{\lambda^2}{4} \,\middle|\, \begin{matrix} -\frac{3}{2} \\ -\frac{1}{2}, 0, \frac{1}{2} \end{matrix}\right) - G_{13}^{31}\left(\frac{\lambda^2}{4} \,\middle|\, \begin{matrix} -\frac{1}{2} \\ -\frac{1}{2}, 0, \frac{1}{2} \end{matrix}\right)\right] \\
&\quad + \frac{8\alpha\lambda}{\sqrt{\pi}} \left[G_{13}^{31}\left(\lambda^2 \,\middle|\, \begin{matrix} -\frac{3}{2} \\ -\frac{1}{2}, 0, \frac{1}{2} \end{matrix}\right) - G_{13}^{31}\left(\lambda^2 \,\middle|\, \begin{matrix} -\frac{1}{2} \\ -\frac{1}{2}, 0, \frac{1}{2} \end{matrix}\right)\right]
\end{aligned}$$

$$\begin{aligned}
\beta_2 &= \int_0^{\pi} sin(2\theta) g(\theta) d\theta \\
&= \int_0^{\pi} sin(2\theta) \sec^2\left(\frac{\theta}{2}\right) e^{-\lambda \tan\left(\frac{\theta}{2}\right)} \left[\frac{\lambda(1-\alpha)}{2} + 2\lambda e^{-\lambda \tan\left(\frac{\theta}{2}\right)}\right] d\theta \\
&= \int_0^{\infty} \left(\frac{4x}{(1+x^2)} - \frac{8x^3}{(1+x^2)^2}\right) \left[(1-\alpha)\lambda e^{-\lambda x} + 2\alpha\lambda e^{-2\lambda x}\right] dx.
\end{aligned}$$

Therefore,

$$\begin{aligned}
\beta_2 &= \frac{2(1-\alpha)\lambda}{\sqrt{\pi}} \left[G_{13}^{31}\left(\frac{\lambda^2}{4} \,\middle|\, \begin{matrix} 0 \\ 0, 0, \frac{1}{2} \end{matrix}\right) - 2G_{13}^{31}\left(\frac{\lambda^2}{4} \,\middle|\, \begin{matrix} -1 \\ 0, 0, \frac{1}{2} \end{matrix}\right)\right] \\
&\quad + \frac{4\alpha\lambda}{\sqrt{\pi}} \left[G_{13}^{31}\left(\lambda^2 \,\middle|\, \begin{matrix} 0 \\ 0, 0, \frac{1}{2} \end{matrix}\right) - 2G_{13}^{31}\left(\lambda^2 \,\middle|\, \begin{matrix} -1 \\ 0, 0, \frac{1}{2} \end{matrix}\right)\right].
\end{aligned}$$

In a similar manner, higher order moments can be obtained. □

4. The Maximum Likelihood Estimation

Within this section, we delve into the process of employing maximum likelihood estimation to determine the model parameters α and λ.

Let $\theta_1, \theta_2, \theta_3, \ldots, \theta_n$ be a random sample of size n from the TSSCED distribution, then the likelihood function is given by

$$\begin{aligned} L(\theta_1, \theta_2, \theta_3, \ldots, \theta_n;\ \alpha, \lambda) &= \prod_{i=1}^{n} g(\theta_i;\ \alpha, \lambda) \\ &= \left(\frac{\lambda}{2}\right)^n \prod_{i=1}^{n} \sec^2\left(\frac{\theta_i}{2}\right) \exp\left(-\lambda \tan\left(\frac{\theta_i}{2}\right)\right) \\ &\quad \left[\alpha\left(\exp\left(-\lambda \tan\left(\frac{\theta_i}{2}\right)\right) - 1\right) + 1\right]; \end{aligned}$$

the log likelihood function is given by

$$\begin{aligned} l &= \log(L) \\ &= n \log\left(\frac{\lambda}{2}\right) + 2\sum_{i=1}^{n} \log\left(\sec\left(\frac{\theta_i}{2}\right)\right) - \lambda \sum_{i=1}^{n} \tan\left(\frac{\theta_i}{2}\right) \\ &\quad + \sum_{i=1}^{n} \log\left[\alpha\left(e^{-\lambda \tan\left(\frac{\theta_i}{2}\right)} - 1\right) + 1\right]. \end{aligned} \tag{12}$$

If the first partial derivative of (12) with respect to parameters α and λ is taken and equalized to zero, then we have the following two normal equations:

$$\frac{\partial l}{\partial \alpha} = \sum_{i=1}^{n} \left[\frac{e^{-\lambda \tan\left(\frac{\theta_i}{2}\right)} - 1}{\alpha\left(e^{-\lambda \tan\left(\frac{\theta_i}{2}\right)} - 1\right) + 1}\right] = 0 \tag{13}$$

$$\frac{\partial l}{\partial \lambda} = \frac{n}{\lambda} - \sum_{i=1}^{n} \tan\left(\frac{\theta_i}{2}\right) - \frac{\lambda\alpha}{2} \sum_{i=1}^{n} \left[\frac{\sec^2\left(\frac{\theta_i}{2}\right) e^{-\lambda \tan\left(\frac{\theta_i}{2}\right)} - 1}{\alpha\left(e^{-\lambda \tan\left(\frac{\theta_i}{2}\right)} - 1\right) + 1}\right] = 0. \tag{14}$$

Due to the presence of nonlinear terms in Equations (13) and (14), it is not feasible to derive closed-form expressions for the maximum likelihood estimators. As a result, analytical solutions are unattainable, leading us to utilize a numerical approach in order to obtain parameter values for α and λ.

5. Simulation Study

Take samples of size: $n = 20, 40, 100, 200,$ and 900.
Step-I: Generating a random sample from a given distribution;
Step-(a): A random variable is generated from the U (0, 1) distribution, say u;
Step-(b): Find the expression for the quantile function for the given distribution (i.e., find the inverse of cumulative distribution function);

Steps (a) and (b) are repeated as many times as the desirable sample size (i.e., replications say N = 10,000);
Step-II: Obtain maximum likelihood estimates of the parameters.

The MLEs of the parameters are obtained by substituting the values obtained from Step-I in log-likelihood function and maximizing;
Step-III: Calculate the average bias, MSE, and MRE.

Let the true value of the parameter be $MSE(\lambda^*) = \frac{1}{N} \sum_{i=1}^{N} (\lambda_i - \lambda^*)^2$ and the MLE be λ^* . Then the average bias, MSE, and MRE of λ^* are given by

$$|Bias(\lambda^*)| = \frac{1}{N}\sum_{i=1}^{N}(|\lambda_i - \lambda^*|), \text{ where } Bias(\lambda^*) = \frac{1}{N}\sum_{i=1}^{N}(\lambda_i - \lambda^*),$$

$$MSE(\lambda^*) = \frac{1}{N}\sum_{i=1}^{N}(\lambda_i - \lambda^*)^2$$

$$MRE(\lambda^*) = \frac{1}{N}\sum_{i=1}^{N}\frac{|(\lambda_i - \lambda^*)|}{\lambda^*}.$$

Similarly, the bias, MSE, and MRE for other parameters are calculated.

The data presented in Table 1 indicate that, as the sample size increases, the absolute bias and MSE of the maximum likelihood estimation (MLE) for α and λ tend to diminish. This trend signifies that the parameter estimates for α and λ are becoming more accurate, precise, and, consequently, consistent.

Table 1. MLE, average bias, MSE, and MRE for α^* and λ^*.

Sample Size		**α**				**λ**		
n		$\alpha = -0.25$				$\lambda = 1.5$		
n	MLE	Bias	MSE	MRE	MLE	Bias	MSE	MRE
20	−0.30923	0.42563	0.25468	−1.70253	1.53668	0.37243	0.24245	0.24829
40	−0.25845	0.3390	0.17890	−1.35599	1.55175	0.30226	0.17154	0.20151
100	−0.23798	0.23241	0.09592	−0.92964	1.54459	0.20985	0.09844	0.13990
200	−0.24235	0.16354	0.04966	−0.65415	1.52372	0.14304	0.04808	0.09536
900	−0.25044	0.07357	0.00858	−0.29429	1.50136	0.06098	0.00595	0.04065
n		$\alpha = -0.75$				$\lambda = 2$		
	MLE	Bias	MSE	MRE	MLE	Bias	MSE	MRE
20	−0.71745	0.27163	0.13031	−0.36217	2.07549	0.37501	0.28395	0.18751
40	−0.73827	0.20850	0.07905	−0.27800	2.04035	0.26774	0.15105	0.13387
100	−0.74988	0.13439	0.02934	−0.17918	2.00860	0.16353	0.04483	0.08177
200	−0.75048	0.09666	0.0149	−0.12888	2.00517	0.11410	0.02079	0.05705
900	−0.75002	0.04551	0.00326	−0.06067	2.00106	0.05308	0.00446	0.02654
n		$\alpha = 0.25$				$\lambda = 2.75$		
	MLE	Bias	MSE	MRE	MLE	Bias	MSE	MRE
20	0.06332	0.46435	0.32862	1.85741	2.60236	0.6671	0.65624	0.24258
40	0.11763	0.38189	0.21671	1.52758	2.66402	0.59805	0.53040	0.21747
100	0.19594	0.29615	0.12576	1.18460	2.76669	0.50778	0.39994	0.18465
200	0.23879	0.23884	0.08486	0.95537	2.75853	0.42811	0.30909	0.15568
900	0.25602	0.19277	0.05951	0.77109	2.75097	0.35724	0.23727	0.12991
n		$\alpha = 0.5$				$\lambda = 3.5$		
	MLE	Bias	MSE	MRE	MLE	Bias	MSE	MRE
20	0.3497	0.43623	0.31876	0.87246	3.32569	0.75798	0.81984	0.21657
40	0.38084	0.36559	0.21933	0.73117	3.38228	0.70477	0.69674	0.20136
100	0.41406	0.29573	0.13587	0.59146	3.42742	0.63041	0.55988	0.18012
200	0.44827	0.24924	0.09391	0.49849	3.46991	0.56018	0.44954	0.16005
900	0.48967	0.16542	0.04037	0.33083	3.51229	0.39465	0.23494	0.11276

Table 1. *Cont.*

Sample Size	α				λ			
n	$\alpha = 0.75$				$\lambda = 4.75$			
	MLE	Bias	MSE	MRE	MLE	Bias	MSE	MRE
20	0.61623	0.36033	0.23862	0.48044	4.44351	0.95696	1.31564	0.20146
40	0.66202	0.29647	0.14938	0.39530	4.56807	0.85815	1.03825	0.18066
100	0.69448	0.23836	0.08797	0.31781	4.68178	0.77811	0.84347	0.16381
200	0.70655	0.20618	0.06435	0.27490	4.71495	0.71606	0.71555	0.15075
900	0.74987	0.14159	0.03241	0.18879	4.70835	0.50387	0.38176	0.10608
n	$\alpha = 1$				$\lambda = 6$			
	MLE	Bias	MSE	MRE	MLE	Bias	MSE	MRE
20	0.84397	0.15603	0.12359	0.15603	5.31865	1.19575	2.13013	0.19929
40	0.87742	0.12258	0.07097	0.12258	5.47974	0.97930	1.51715	0.16322
100	0.90301	0.09699	0.04792	0.09699	5.58728	0.74017	0.99825	0.12336
200	0.92618	0.07382	0.03465	0.07382	5.69486	0.55759	0.67826	0.09293
900	0.97800	0.02200	0.00591	0.02200	5.88721	0.22750	0.13504	0.03792

6. Application

In river environments, pebbles are often subjected to a variety of hydraulic forces, such as water flow, turbulence, and sediment transport. These forces can change the orientation of pebbles and cause them to align in certain directions. Various studies have shown that pebble orientation in river environments can be influenced by a variety of factors, including the direction and velocity of water flow, the size and shape of the pebbles, the slope of the riverbed, and the presence of other sediment particles. In this study, to illustrate the potentiality of the proposed model, we consider one such dataset from Krumbein in [29]; this dataset consists of a direction of 100 washout pebbles from a lake Wisconsin outwash terrace along Fox River near Cary, Illinois.

Data: Orientations of pebbles: Horizontal axes of 100 outwash pebbles from a lake Wisconsin outwash terrace along Fox River near Cary, Illinois.

To check the goodness-of-fit for the proposed distribution and its baseline distribution to the above-mentioned dataset, we compute statistics, log-likelihood, AIC (Akaike information criterion), CAIC (corrected Akaike information criterion), BIC (Bayesian information criterion), and HQIC (Hannan–Quinn information criterion). Table 2 shows the parameter estimator's results along with the standard error of the wrapped exponential (WE), wrapped Lindley (WL), wrapped modified Lindley (WML), wrapped xgamma (WRXG) transmuted wrapped exponential (TWE), stereographic semicircular exponential (SSCED) and transmuted stereographic semicircular exponential (TSSCED), stereographic semicircular half logistic (SSCHLD), and stereographic semicircular quasi Lindley (SSCQLD). Table 3 shows the corresponding log-likelihood, AIC, CAIC, BIC, HQIC, and Kolmogorov–Sminorov (KS) statistic. Table 4 shows a summary of statistics/values of log-likelihood, AIC, CAIC, BIC, HQIC, and KS statistic for the pebbles dataset.

In Figure 7 we present Circular plot of pebbles data set (left and right).

Table 2. One hundred outwash pebbles (Fisher-B8).

Direction	0	20	40	60	80	100	120	140	160
Frequency	16	13	9	14	9	14	12	6	7

In the following Figure 8 we provide the rose diagram of orientations of pebbles.

Table 3. MLEs and their standard errors for pebbles data (Fisher-B8 data).

Model	$\hat{\lambda}$ (SE)	$\hat{\alpha}$ (SE)
WE (α)	0.7925781 (0.08714681)	–
TWE (λ, α)	0.9076947 (0.1091980)	−0.2786174 (0.1737912)
SSCEXPD (λ)	0.8707031 (0.0870702)	–
TSSCED (λ, α)	0.6486455 (0.1179918)	0.5616030 (0.2311657)
SSCHLD (α)	0.8724609 (0.07618154)	–
SSCQLD (σ, λ)	37.410889 (114.4836132)	0.8929941 (0.11080331)
WRXG (λ)	1.506348 (0.1119663)	–
WML (λ)	0.8916573 (0.07748228)	–
WL (λ)	1.181641 (0.09453908)	–

Table 4. Summary of statistics/values of log-likelihood, AIC, CAIC, BIC, HQIC, and KS statistic for the pebbles dataset.

Model	LL	AIC	CAIC	BIC	HQIC	KS (p-Value)
TSSCED (λ, α)	−103.8731	211.7461	211.8698	216.9565	213.8449	0.146 (0.06598)
SSCEXPD (λ)	−106.4283	214.8566	214.8974	217.4617	215.9109	0.16 (0.03195)
WE (λ)	−119.1116	240.2282	240.624	242.8284	241.2776	0.27892 (0.00003)
TWE (λ, α)	−188.1661	240.3323	240.456	245.5426	242.441	0.169 (0.006355)
SSCLHD (α)	−115.5355	233.071	233.1118	235.6762	234.1254	0.20069 (0.0006346)
SSCQLD (σ, λ)	−106.4473	216.8946	217.0183	222.105	219.0033	0.16 (0.1195)
WRXG (λ)	−114.8499	231.6999	231.7407	234.3051	232.7543	0.1823 (0.002597)
WML (λ)	−121.4082	244.8164	244.8572	247.4215	245.8707	0.16 (0.01195)
WL (λ)	−117.3191	236.6382	236.679	239.2434	237.6926	0.16419 (0.009111)

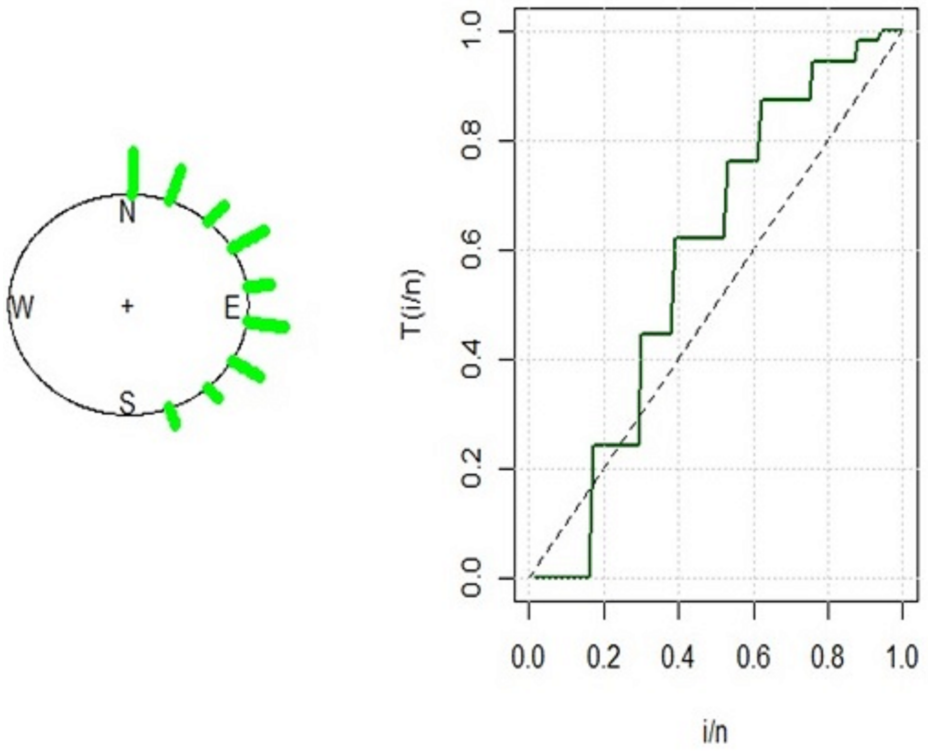

Figure 7. (**left**) Circular plot of pebbles data set (FisherB8) and (**right**) TTT-plot for pebbles dataset.

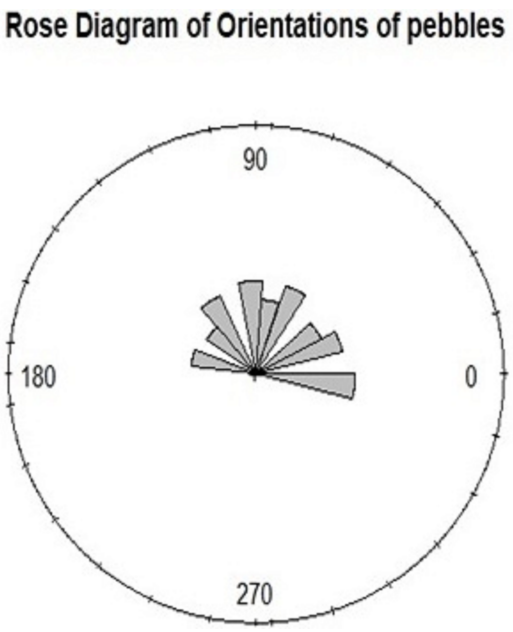

Figure 8. Rose diagram of orientations of pebbles

It can be observed that the transmuted stereographic semicircular distribution has minimum values of AIC, CAIC, BIC, HQIC, and a higher *p*-value, thus leading to the conclusion that the proposed distribution achieves a better fit than other competing models. In Figure 9 we present the fitted density, distribution, Q-Q, and P-P plots of the proposed model for pebbles data.

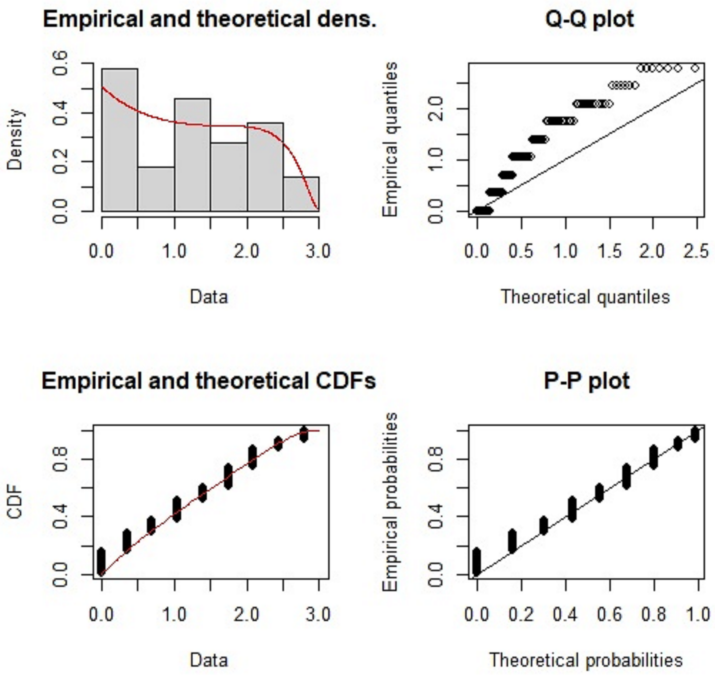

Figure 9. Fitted density, distribution, Q-Q, and P-P plots of the proposed model for pebbles data.

In Figure 10 we provide estimated density function and estimated cumulative distribution function of the proposed model TSSCED.

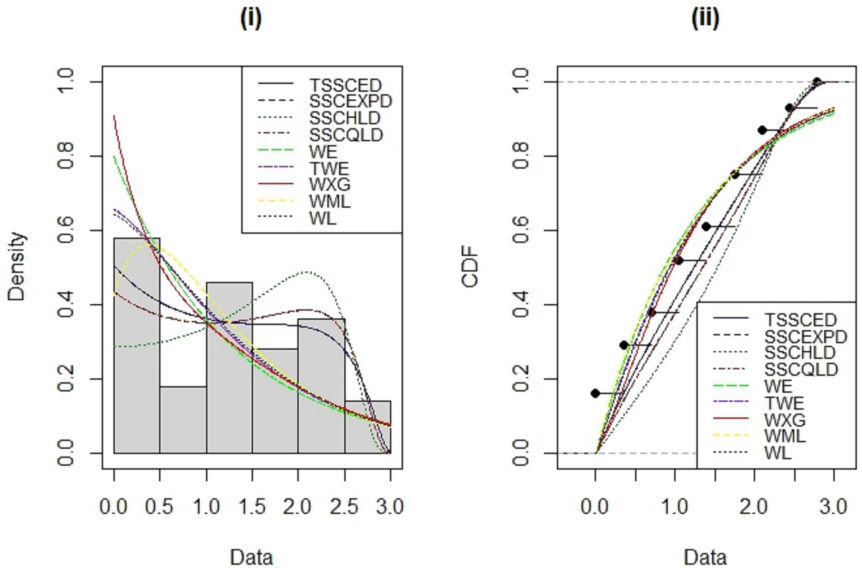

Figure 10. Plots of (**i**) estimated density function and (**ii**) estimated cumulative distribution function of the proposed model TSSCED with those of the other competitive models for pebbles data.

7. Conclusions

This article introduced a novel semicircular distribution using the widely recognized Quadratic Rank Transmutation Map (QRTM) technique applied to the stereographic semicircular exponential distribution. We derive the closed-form expressions for the first two trigonometric moments and employ the maximum likelihood method to estimate the parameters of this newly proposed distribution. Moreover, we validate the practical utility of our model by applying it to real-world data sets. Our observations reveal that both the proposed distribution and its underlying distribution offer a superior fit compared to various other distributions, including the wrapped exponential distribution (Jammalamadaka and Kozubowski in [11]), the wrapped Lindley (Joshi et al. in [30]), the wrapped xgamma distribution (Hazem-AI-Mofleh et al. in [31]), the wrapped modified Lindley distribution (Christophe et al. in [32]), the stereographic semicircular half logistic distribution (P. Yedlapalli et al. in [23]), the stereographic semicircular quasi Lindley distribution (P. Yedlapalli et al. in [22]), and the transmuted wrapped exponential distribution (Abdullah Yilmaz in [21]). Furthermore, our findings indicate that the transmuted distribution exhibits greater flexibility than its base distribution.

Areas of Future Exploration: (i) Circular regression: Extend circular regression techniques to semicircular data, enabling the modeling of relationships between circular and linear variables in mixed data types. (ii) Bayesian approaches: Explore Bayesian approaches for semicircular data analysis, which can provide a robust framework for parameter estimation, uncertainty quantification, and model comparison [33,34]. (iii) Investigate modeling semicircular data with multiple modes, which is common in many real-world scenarios, such as directional bimodality.

Author Contributions: Conceptualization, P.Y. and G.N.V.K.; methodology, P.Y. and G.N.V.K.; software, P.Y., W.B. and G.N.V.K.; validation, W.B., A.K. and N.M.; formal analysis, W.B., A.K. and N.M.; investigation, P.Y., W.B., A.K. and N.M.; resources, W.B., A.K. and N.M.; data curation, P.Y., G.N.V.K., W.B., A.K. and N.M.; writing—original draft preparation, P.Y., G.N.V.K., W.B., A.K. and N.M.; writing—review and editing, P.Y., G.N.V.K., W.B., A.K. and N.M.; visualization, W.B. and N.M.; supervision, W.B., A.K. and N.M.; project administration, W.B. and N.M.; funding acquisition, W.B. All authors have read and agreed to the published version of the manuscript.

Funding: This research received no external funding.

Data Availability Statement: All data required for this research are included within the paper.

Acknowledgments: The authors W. Boulila, A. Koubaa and N. Mlaiki would like to thank the Prince Sultan University for paying the publication fees for this work through RIOTU LAB.

Conflicts of Interest: The authors declare no conflict of interest.

References

1. Hamasha, M.M. Practitioner advice: Approximation of the cumulative density of left-sided truncated normal distribution using logistic function and its implementation in Microsoft Excel. *Qual. Eng.* **2017**, *29*, 322–328. [CrossRef]
2. Khan, M.A.; Meetei, M.Z.; Shah, K.; Abdeljawad, T.; Alshahrani, M.Y. Modeling the monkeypox infection using the Mittag–Leffler kernel. *Open Phys.* **2023**, *21*, 20230111. [CrossRef]
3. Kamal, S.; Rohul, A.; Thabet, A. Utilization of Haar wavelet collocation technique for fractal-fractional order problem. *Heliyon* **2023**, *9*, e17123. [CrossRef]
4. Albert, W.M.; Ingram, O. A New Method for Adding a parameter to a family of Distributions with Applications to the Exponential and Weibull Families. *Biometrika* **1997**, *84*, 641–652.
5. Shaw, W.; Buckley, I. The Alchemy of Probability Distributions. Beyond Gram-Charlier Expansions and A Skew-Kurtotic –Normal Distribution from a Rank Transmutation Map. *arXiv* **2007**, arXiv:0901.0434.
6. Merovci, F. Transmuted Lindley Distribution. *Int. J. Open Probl. Compt. Math.* **2013**, *6*, 64–72. [CrossRef]
7. Merovci, F.; Ibrahim, E. Transmuted Lindley-geometric distribution and its applications. *J. Stat. Appl. Probab.* **2014**, *3*, 77–91. [CrossRef]
8. Kemaloglu, S.A.; Yilmaz, M. Transmuted two-parameter Lindley distribution. *Commun. Stat.-Theory Methods* **2017**, *46*, 11866–11879. [CrossRef]
9. Rao, J.S.; Gupta, S. *Topics in Circular Statistics*; World Scientific Press: Singapore, 2001.
10. Jammalamadaka, S.R.; Kozubowski, T.J. A new family of circular models: The wrapped Laplace distributions. *Adv. Appl. Stat.* **2003**, *3*, 77–103.
11. Jammalamadaka, S.R.; Kozubowski, T.J. New Families of Wrapped distributions for modeling Skew circular data. *Commun. Stat.-Theory Methods* **2004**, *33*, 2059–2074. [CrossRef]
12. Abe, T.; Shimizu, K.; Pewsey, A. Symmetric unimodel models for directional data motivated by inverse stereographic projection. *J. Jpn. Stat. Soc.* **2020**, *40*, 45–61. [CrossRef]
13. Minh, D.L.P.; Farnum, N.R. Using bilinear transformations to induce probability distributions. *Commun. Stat.-Theory Methods* **2003**, *32*, 1–9. [CrossRef]
14. Jones, M.C.; Pewsey, A. A family of symmetric distributions on the circle. *J. Am. Stat. Assoc.* **2005**, *100*, 1422–1428. [CrossRef]
15. Yedlapalli, P.; Girija, S.V.S.; Rao, A.V.D. On Construction of Stereographic Semicircular models. *J. Appl. Probab. Stat.* **2013**, *8*, 75–90.
16. Rao, A.V.D.; Sharma, I.R.; Girija, S.V.S. On wrapped version of some life testing models. *Commun. Stat.-Theory Methods* **2007**, *36*, 2027–2035. [CrossRef]
17. Arnold, B.; Sen, C.; Gupta, A. Probability distributions and statistical inference for axial data. *Environ. Ecol. Stat.* **2016**, *13*, 271–285. [CrossRef]
18. Rambli, A.; Mohamed, I.B.; Shimizu, K.; Khalidin, N. Outlier detection in a new half-circular distribution. In Proceedings of the AIP Conference Proceedings, Selangor, Malaysia, 24–26 November 2015; p. 050018. [CrossRef]
19. Ali, H.A. A half circular distribution for modeling the posterior corneal curvature. *Commun.-Stat.-Theory Methods* **2017**, *47*, 3118–3124. [CrossRef]
20. Rambli, A.; Mohamed, I.B.; Shimizu, K.; Khalidin, N. A Half-Circular Distribution on a Circle. *Sains Malays.* **2019**, *48*, 887–892. [CrossRef]
21. Abdullah, Y.; Cenker, B. A new wrapped exponential distribution. *Math. Sci.* **2018**, *12*, 285–293. [CrossRef]
22. Yedlapalli, P.; Girija, S.V.S.; Akkayajhula, V.D.R.; Sastry, K.L.N. On Stereographic Semicircular Quasi Lindley Distribution. *J. New Results Sci. (JNRS)* **2016**, *8*, 6–13.
23. Yedlapalli, P.; Subrahmanyam, P.S.; Girija, S.V.S.; Rao, A.V.D. Stereographic Semicircular Half Logistic Distribution. *Int. J. Pure Appl. Math. (IJPAM)* **2017**, *113*, 142–150.
24. Yedlapalli, P.; Girija, S.V.S.; Rao, A.V.D.; Sastry, K.L.N. A New Family of Semicircular and Circular Arc Tan-Exponential Type Distributions. *Thai J. Math.* **2020**, *18*, 775–781.
25. Ayesha, I.; Azeem, A.; Hanif, M. Half circular modified burr-III distribution, application with different estimation methods. *PLoS ONE* **2022**, *17*, e0261901. [CrossRef]
26. Alldredge, J.R.; Mahtab, M.A.; Panek, L.A. Statistical analysis of axial data. *J. Geol.* **1974**, *82*, 519–524. [CrossRef]
27. Mardia, K.V.; Jupp, P.E. *Directional Statistics*, 2nd ed.; John Wiley Sons, Ltd.: Hoboken, NJ, USA, 2000.
28. Gradshteyn, R. *Table of Integrals, Series and Products*, 7th ed.; Academic Press: Cambridge, MA, USA, 2007.
29. Krumbein, W.C. Preferred Orinetation of Pebbles in Sedimentary Deposits. *J. Geol.* **1939**, *47*, 673–706. [CrossRef]
30. Joshi, S.; Jose, K.K. Wrapped Lindley Distribution. *Commun. Stat.-Theory Methods* **2018**, *47*, 1013–1021. [CrossRef]
31. Al-Mofleh, H.; Sen, S. The wrapped xgamma distribution for modeling circular data appearing in geological context. *arXiv* **2019**, arXiv:1903.00177.
32. Christophe, C.; Lishamol, T.; Meenu, J. Wrapped modified Lindley distribution. *J. Stat. Manag. Syst.* **2021**, *24*, 1025–1040.

33. Boulila, W.; Farah, I.; Ettabaa, K.; Solaiman, B.; Ghézala, H. Improving spatiotemporal change detection: A high level fusion approach for discovering uncertain knowledge from satellite image databases. *Icdm* **2009**, *9*, 222–227.
34. Ferchichi, A.; Boulila, W.; Farah, I. Propagating aleatory and epistemic uncertainty in land cover change prediction process. *Ecol. Inform.* **2017**, *37*, 24–37. [CrossRef]